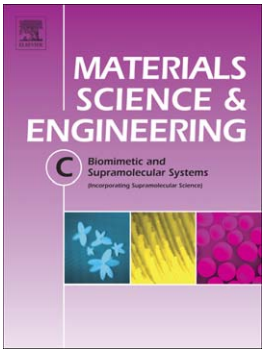

Studies on L-HISTIDINE CAPPED AG AND AU NANOPARTICLES FOR DOPAMINE DETECTION

CHANDRASEKARAN NIVEDHINI ISWARYA, S.C.G. KIRUBA DANIEL, MUTHUSAMY SIVAKUMAR

PII: S0928-4931(16)32350-5
DOI: DOI:10.1016/J.MSEC.2016.11.102
REFERENCE: MSC 7156

TO APPEAR IN: *Materials Science & Engineering C*

RECEIVED DATE: 25 JUNE 2016
REVISED DATE: 13 SEPTEMBER 2016
ACCEPTED DATE: 24 NOVEMBER 2016

Please cite this article as: Chandrasekaran Nivedhini Iswarya, S.C.G. Kiruba Daniel, Muthusamy Sivakumar, Studies on L-HISTIDINE CAPPED AG AND AU NANOPARTICLES FOR DOPAMINE DETECTION, *Materials Science & Engineering C* (2016), DOI:10.1016/J.MSEC.2016.11.102

Studies on L-Histidine capped Ag and Au nanoparticles for dopamine detection

Chandrasekaran Nivedhini Iswarya[1*], *S.C.G.Kiruba Daniel*[1], *Muthusamy Sivakumar*[1 ,2#]

[1]*Division of Nanoscience and Technology,* [2]*Department of chemistry,*

Anna University-BIT campus, Tiruchirappalli-620024, India.

[#]*Corresponding author:* Tel: +91-431-240-7959 Email: muthusiva@gmail.com

[*]*Present Address: Department of Chemical Engineering, National Institute of Technology, Tiruchirappalli-620015, India.*

Abstract

This work demonstrates the effective surface functionalization of Ag, Au and bimetallic Ag-Au nanoparticles using L-Histidine for colorimetric detection of dopamine(DA) which plays majorly in recognizing the neurological disorder. L-Histidine (L-His) capped Ag, Au, and bimetallic Ag-Au nanoparticles are characterized using physico-chemical techniques. The optical behaviour of nanoparticles has been analysed at various time intervals using UV-Vis absorption spectroscopy. FT-IR results provide the evidence of chemical bonding between L-Histidine and metal nanoparticles. Its structure with the capping of L-His was clearly shown in HR-TEM images. The average size of nanoparticles has calculated from TEM image fringes are 11 nm, 5 nm and 6.5 nm respectively, matches with crystals size calculated from X-Ray diffraction pattern. Enhanced optical nature of nanoparticles provides the best platform to develop a colorimetric-based biosensor for DA detection. After addition of DA, a rapid colour change has been noted in colloids of nanoparticles. The substantial changes in absorbance and λ_{max} in metal nanoparticles respect to DA concentration have been observed and formulated. This is one of the successive methods for trace level determination of DA and will be going to a significant material for designing biosensor to determine DA in real extracellular body fluids.

Keyword: L-Histidine, Dopamine sensing, Ag, Au,Bimetallic Nanoparticles, Biosensor

1.Introduction

Recently metal nanoparticles became more eye-catching for their excellence in detection and imaging purpose[1]. Currently, many types of research on ligand-protected metal nanoparticles are being achieved and investigated. The interesting electro-optical behaviourism of interconnected biomolecules and metallic nanoparticles bring more significance in developing the biosensing materials[2–7]. Among various metal nanoparticles, Au and Ag attract many researchers interest owing to their properties like optical chirality, quantized charging behaviour and photoluminescence along with a wide range of application in the field of sensing, catalysis and labelling[8–19].

Among various amino acids L-Histidine (L-His) is a one with aromatic nitrogen and imidazole side chain. Due to its extreme biochemical importance, it is used in various biological process and medical applications[20].The three main sites in L-His, which participated in metal adsorption arethe carboxylic group, imidazole nitrogen atom, and amino group[21]. Owing to the presence of this sites, L-His acts as one of the strongest metal ion binders. Many investigations have been reported to explore the interaction of L-His with metals and metal oxides like Cd, Fe, Zn, Co, ZnO,Fe_3O_4[22–26].

Dopamine (DA) is a catecholamine neurotransmitter, which plays a crucial role as chemical messengers in central nervous system, hormonal, cardiovascular and renal systems. Recently, many attentions are paid to trace level determination of DA, because small changes in concentration coupled with various disorders like Alzheimer's disease, epilepsy, Parkinson's disease, schizophrenia, and pheochromocytoma etc. The selective and sensitive approach for DA level determination is vital for diagnosing diseases. It has been shown that metal nanoparticles having better sensing activity[27–29]. Metal nanoparticles like magnetic Fe_3O_4 with Au nanoparticles have been utilized for DA sensing and detection [30].

In this present work, the detection of DA using L-His capped metal (Ag, Au) nanoparticles has been studied by analysing the SPR peak shift after addition of DA.The optical properties, crystalline pattern and the morphological structure of L-His capped metal nanoparticles(Ag, Au, Ag-Au) have been investigated. And the comparative DA sensing behaviours of synthesized metal nanoparticles has been studied at the different concentration of DA. The relation between the wavelength of maximum absorbance (λ_{max}), absorbance, and DA concentration are formulated based on sensing property. So for many electrodes and colorimetry based DA sensor has been developed[31]. To our knowledge, it is a simple, easy

and handy method for detection of DA concentration using biomolecules assisted bi-metallic nanoparticles.

2.Experimental Procedure

2.1. Materials

Aurochloric acid ($HAuCl_4$) and Silver nitrate ($AgNO_3$)were purchased from Sigma-Aldrich India and used as initial precursors for synthesizing L-His capped Ag, Au, and Ag-Au nanoparticles. L-Histidine ($C_6H_9N_3O_2$) and Sodium hydroxide (NaOH) were obtained from Merck Specialities Private Limited India. All chemical reagents of analytical grade areused as received without any further purification.

2.2. Synthesis of L-Histidine capped nanoparticles

L-His solution has been prepared by dissolving 10 mM L-His in 100mL double distilled water (DD). By dissolving 30mM of $AgNO_3$ and $HAuCl_4$ in 2mL DD respectively. Like the same NaOH solution has been prepared by dissolving 25 mM of NaOH in 50 mL DD. Finally, the preparation of three different nanoparticles has shown in table 1.

Table 1: Synthesis of nanoparticles with various parameters

Sample Name	Nanoparticles	L-His Solution	Ag^+Solution	Au^{3+} Solution	NaOH Solution	Colour change
i	L-His capped Ag	30 mL	500 µL	-	10 mL	Yellow
ii	L-His capped Au	30 mL	-	500 µL	10 mL	Pink
iii	L-His capped Ag-Au	30 mL	500 µL	500 µL	10 mL	Orange

These three different samples are maintained at 60^0 C, and the reaction has been terminated after attaining the respective colour changes as noted in Table 1.

2.3. Procedure for dopamine sensing

Different concentrations of DA have been prepared by dissolving 10 µM, 15 µM, 20 µM and 25 µMin 100 µL of DD respectively and are tested against L-His based Ag, Au and Ag-Au nanoparticles. Real-time colour change has been noted from yellow to dark yellow for Sample i. Similarly, visible colour change from pink to violet and orange to red respectively occurs for Sample ii and Sample iii after addition of DA at different concentration.

2.4. Characterization

Optical absorption spectra have been recorded using a JASCO V-650 spectrophotometer in theUV-Visible wavelength range of 200nm-900 nm and images of respective colour changes during reactions has been photographed with a Canon digital camera. The surface morphology has been studied using Atomic force microscope (AFM Park System,100XE) at different magnifications range with silicon nitride cantilever tip height 10–12 nm in the contact mode.TEM samples are prepared by dropping solution onto a carbon coated copper grid (3 mm, 200 mesh), and images have been captured with Tecnai (FEI)high -resolution transmission electron microscope (HR-TEM). Thecrystallinity and phase changes have been obtained by Rigaku Ultima III X-ray diffraction (XRD) with Cu-K α radiation (1.500 Å, 40 kV, 30 mA). The fingerprints of functional group bindings are recorded in the spectral range of 400cm^{-1} - 4000 cm^{-1} using a PerkinElmer FTIR spectrophotometer.

3. Results and discussion

3.1. Spectral characteristics

UV-Vis spectra for different nanoparticles are measured at different time intervals during the experimental procedure are shown in Fig. 1. The surface plasmon resonance (SPR) peak of L-His capped Ag [Fig. 1(A)] nanoparticles and L-His capped Au [Fig.1(B)]are at 415 nm and 539 nm respectively. Whereas for L-His capped Ag-Au nanoparticles [Fig. 1(C)], the broad SPR peak exhibits in the range of 430-540 nm confirms the presence of both Ag and Au nanoparticles. Similarly, there is an existence of L-His peak in all three synthesised nanoparticles at 282 nm,283 nm,279 nm, respectively shows the capping behaviour of L-His above the nanoparticles. This proves the L-His acts as both capping and reducing agent. As time increases, nucleation starts and further growth of nanoparticles taken place which is directly related to the absorption as well as yield. After attaining the growth, absorption gets saturated with the maximum yield at 60 min, 120 min and 60 min for Ag, Au, and Ag-Au nanoparticle respectively shown in Fig.S1(see supplementary). This show the ions get reduced completely and further capping agent prevents the aggregation of respective nanoparticles.

The available chemical bonds and its bindings between L-His and metal nanoparticles have been studied using Fourier transform infrared spectroscopy. In the spectrum of L-His Fig 2(A), the absorption position at 675-750 cm^{-1}, 1124 cm^{-1}, 1404 cm^{-1}, 1490 cm^{-1},

1640 cm^{-1}, 2080 cm^{-1}, 3200-3500 cm^{-1} corresponds to bending vibration (δ) of sp^2 CH group, stretching vibration (ν) of CN in imidazole group, symmetric stretching (ν_s) mode of COO^- group, symmetric NH bend, ν(C=C), ν(N–H) and ν(O–H) of H_2O, respectively[32–34]. In Fig 2(B), the presence of COO^- group at 1404 cm^{-1}in L-His has been shifted slightly to 1385 cm^{-1}, 1384 cm^{-1}, and 1388 cm^{-1} in L-His capped Ag, Au, Ag-Au nanoparticles respectively, indicates the interaction of carboxylic group of one L-His molecule with amine group presents in neighbour L-His molecule. Whereas the vibrations in the spectral position 1124 cm^{-1} and 1490 cm^{-1} in L-His are absent in metal nanoparticle spectra, proves the adsorption of L-His on the metal surface through amine group and nitrogen atom present in the imidazole group. This result indicates the binding as well as the capping of L-His over metal nanoparticles.

3.2. XRD Characteristics

XRD pattern of L-His capped Ag, Au, Ag-Au nanoparticles has shown in the Fig. 3. This graph shows diffraction pattern of L-His capped Ag nanoparticles having a face-centered cubic lattice matches with JCPDS No: 01-087-0597.Similarly, the XRD pattern of L-His capped Au nanoparticle matches with the JCPDS No: 00-002-1095 and having a cubic system of the face-centered lattice. Whereas inthe diffraction pattern of L-His capped Ag-Au nanoparticles, some peaks marked with (#) are matches with the JCPDS No: 00-041-1402 corresponds to the Ag, hexagonal systems having primitive lattice. While some others are matches with the JCPDS No: 00-004-0784, which corresponds to the Au, cubic systems having a face-centred lattice. The mean crystal size has calculated using Debye - Scherrer's formulae $D = 0.9\lambda/\beta\cos\theta$ where λ is the used x-ray wavelength and β is Full Width at Half Maximum (FWHM). The average crystal size of L-His capped Ag, Au. Ag-Au nanoparticles are calculated as 9.76 nm, 5.83 nm, and 6.71 nm respectively.

3.3. Microscopic analysis

Fig.4 gives the topographical image of L-His capped Ag, Au, Ag-Au nanoparticles have taken in 2 x 2 μm scale using AFM in contact mode at atip height of 10 nm. Then surface scanning of nanoparticle has been done for several contact times. Fig 4(A) confirms the spherical shape of L-His capped Ag nanoparticles with a size less than10 nm. And the presence of L-his keeps the nanoparticles in same uniformity with proper distance. This proves the L-His acts as a capping over the nanoparticles, which prevents particle aggregation. The particle size has measured using line profile determination is in the range

between 10-16 nm. Likewise, the Fig 4(B) shows the irregular spherical form of L-his functionalized Au nanoparticles. Average particle size from line profile data is nearly to 7 nm. And the height of the nanoparticles is nearly to 2 nm. The image further confirms the spatial uniformity between nanoparticles is due to the presence of L-His. Similarly, Fig 4(C) provides the 2D and 3Dinformation of L-His functionalized bimetallic Ag-Au nanoparticles. It clearly reveals the spherical nature of nanoparticles. Moreover, few nanoparticles of big size around 300 nm show the aggregation between Ag and Au nanoparticles i.e. bimetallic nature. And the height of those lies nearly to 7 nm. This is because of agglomeration is seen between two different metal nanoparticles. Here, the particle size lies in the range between 5-12 nm.

HR-TEM images provide an additional information regarding the morphological appearance of nanoparticles in presence of L-His (Fig. 5). From the Fig 5(A), it is clearly seen that dark colour same sized Ag nanoparticles are capped and interconnected by light colour L-His materials. Also, this type interaction resembles in L-His capped Au and Ag-Au nanoparticles, which are shown in Fig. 5(D) and 5(G). Similar kind of interconnection between metal nanoparticles and aminoacids has been reported[35,36].Both Ag and Au nanoparticles are in different size, distributes randomly in the image(Fig. 5(H). And these metals are held together with the help of L-His.Fig. 5(B),5(E)and 5(H) shows the images in scale range of 10 nm for L-His functionalized Ag, Au, bimetallic Ag-Au nanoparticles respectively. The average size of nanoparticles is determined using particle size distribution (Fig. 5(C), 5(F) and 5(I)). The mean particle diameter is found to be 11 nm, 5 nm, and 6.5 nm respectively.

From selected area electron diffraction (SAED) pattern, the crystalline nature of samplesis confirmed. The calculated lattice fringe spacing values are matched with the standard JCPDS data respectively (Fig. 6). This once again proves the crystallinity structure of nanoparticles. The particle size has calculated from HR-TEM slightly greater from the crystal size calculated using XRD. This because of the group of crystals forms a particle. Fig 6(A),6(B) and 6(C) provides the image capture at the scale of 5 nm and SAED pattern respectively.

3.4. Formation mechanism

The alkaline environment is provided by NaOH, to enhance the electron donating property of L-His.Fig.7. shows products of L-His in alkaline solution are imidazole, carbon

dioxide, ammonia, formic acid, and sodium nitrate has been reported[37]. The pH of the initial solution is 11 (basic) whereas for thefinalsolution, it reduces due to the formation of formic acid. Finally, metal nanoparticles are formed because of redox reaction between metal ions and L-His. Excess L-His in the solution forms capping over metal nanoparticles which prevent aggregation. This shows both capping and reducing activities of L-His.

3.5. Dopamine sensing activity

The shift in SPR of nanoparticles after addition of DA at various concentration has shown in Fig 8. The SPR peak of L-His capped Ag nanoparticles [Fig 8(A)] shift accordingly to DA concentration. This because of changes were seen in nanoparticles morphology (size and shape) after addition of DA[38].And a visible colour changes has beenobserved inthe sample I from light yellow to dark yellow. The inset in Fig. 8(A) shows the photograph of samples taken before and after addition of DA.Light yellow colour belongs to clear L-His capped Ag nanoparticles and dark yellow goes to DA added L-His functionalized Ag nanoparticles. It is clearly seen that shift in SPR peak of L-His capped Ag nanoparticles from 425 nm to 430 nm, 445 nm, 475 nm and 485 nm respectively for 10 µM, 15µM, 20 µM and 25 µM of DA concentration. And this depicts the increasing DA concentration, shift the SPR peak towards red wavelength region.Fig.8(B) shows the plot between the logarithmic value of DA concentration with λ_{max} and themaximum absorbance of L-His capped Ag nanoparticles withDA. This spectral data provides,the increase in DA concentration into L-His capped Ag nanoparticles increases the wavelength as well as maximum absorbance. Therefore the logarithmic value of DA concentration is directly proportional to both the maximum absorbance and λ_{max}. These parameters are related to the equation

$$\lambda_{max} = 143.2(\log[DA])^2 + 1522\log[DA] + 4460 \quad (1)$$

$$A|_{\lambda max} = 5.09(\log[DA])^2 + 51.23\log[DA] + 128.9 \quad (2)$$

where λ_{max} is the wavelength in nm corresponding to the maximum absorbance,$A|_{\lambda max}$is maximum absorbance value and [DA] concentration of Dopamine.

Similarly, Fig. 8(C) gives the SPR peak shift of L-His capped Au nanoparticles from 530 nm to 425 nm for all concentration of DA. Here the addition of DA shifts the SPR to the blue region, whereas the concentration of DA has no effect on SPR shift. The inset in Fig. 8(C) provides the photograph of sample ii taken before and after addition of DA are pink and light red respectively.In Fig. 8(D), the increasing DA concentration in L-His capped Au

nanoparticles increases the maximum absorbance value. But λ_{max} has no effect on DA concentration.Therefore the logarithmic value of DA concentration is directly proportional to the maximum absorbance.And the relation is noted down in theequation based on obtained graph.

$$\lambda_{max} = 425 \quad (3)$$

$$A|_{\lambda max} = 0.25\,(\log[DA])^2 + 2.54\log[DA] + 6.81 \quad (4)$$

Effect of DA concentration in L-His capped Ag-Au bimetallic nanoparticles has shown in Fig. 8(E). The SPR peak shiftsfrom a broad hump region 450-520 nm to 435 nm, 425 nm, 420 nm and 410 nm for 10 µM, 15 µM, 20 µM and 25 µM of DA concentration respectively. This depicts the blue region SPR shift has taken place while adding DA of different concentration to the nanoparticles.In Fig.8(F), the increase in DA concentration into L-His capped Ag-Au nanoparticles increases the maximum absorbance but decreases the λ_{max}. The logarithmic value of DA concentration is directly proportional to the absorbance unit at amaximum wavelength, whereas inversely proportional to the wavelength of maximum absorbance.And here relation between the DA concentration with that of maximum absorbance and λ_{max}wasgiven by

$$\lambda_{max} = -120.5\,(\log[DA])^2 + 1206\log[DA] - 2886 \quad (5)$$

$$A|_{\lambda max} = 0.24\log[DA] + 1.32 \quad (6)$$

4. Conclusion

A simple and efficient strategy for the synthesis of Ag, Au, and bimetallic Ag-Au nanoparticles interconnected with L-His has discussed. Since the role of L-His as both reducing and capping agent are clearly proved with FT-IR spectra and HR-TEM. The synthesised colloidal solution are stable in normal environmental condition. The optical absorption peak confirmed the formation of metal nanoparticles. The average diameter of L-His capped Ag, Au, Ag-Au nanoparticles are 11 nm, 5 nm, and 6.5 nm respectively has been calculated from TEM images and also matches with the XRD crystalline size. The imidazole group of L-His is attached to the surface of nanoparticles, which confirmed from FT-IR spectrum. This shows the formation of hydrogen bonds between the free group of L-His and results in a network pattern. Detection of DA has been achieved by UV-Vis Absorption spectra, provides the various SPR peak shift corresponds to

the different concentration of DA in nanoparticles. The further relation has formulated between wavelength and absorbance with concentration of DA. Hence, this basic finding would be utilised for further identification of imbalanced DA concentration in body fluids, which cause serious neuro disorder.

Acknowledgement:

One of the authors (CN) in this work was supported by the TEQIP phase II as teaching assistantship funding from Bharathidasan Institute of Technology, Anna University, Tiruchirappalli- 620024, India

Reference

[1] E. Katz, I. Willner, Integrated nanoparticle--biomolecule hybrid systems: synthesis, properties, and applications, Angew. Chemie Int. Ed. 43 (2004) 6042–6108.

[2] F. Bertorelle, R. Hamouda, D. Rayane, M. Broyer, R. Antoine, P. Dugourd, L. Gell, A. Kulesza, R. Mitric, V. Bonacic-Koutecky, Synthesis, characterization and optical properties of low nuclearity liganded silver clusters: Ag 31 (SG) 19 and Ag 15 (SG) 11, Nanoscale. 5 (2013) 5637–5643.

[3] Y. Cui, Y. Wang, R. Liu, Z. Sun, Y. Wei, Y. Zhao, X. Gao, Serial silver clusters biomineralized by one peptide, ACS Nano. 5 (2011) 8684–8689.

[4] S. Kumar, M.D. Bolan, T.P. Bigioni, Glutathione-stabilized magic-number silver cluster compounds, J. Am. Chem. Soc. 132 (2010) 13141–13143.

[5] T.U.B. Rao, B. Nataraju, T. Pradeep, Ag9 quantum cluster through a solid-state route, J. Am. Chem. Soc. 132 (2010) 16304–16307.

[6] L. Shang, S. Dong, G.U. Nienhaus, Ultra-small fluorescent metal nanoclusters: synthesis and biological applications, Nano Today. 6 (2011) 401–418.

[7] J. Yu, S. Choi, C.I. Richards, Y. Antoku, R.M. Dickson, Live cell surface labeling with fluorescent Ag nanocluster conjugates, Photochem. Photobiol. 84 (2008) 1435–1439.

[8] J. Zheng, P.R. Nicovich, R.M. Dickson, Highly fluorescent noble metal quantum dots, Annu. Rev. Phys. Chem. 58 (2007) 409.

[9] L.A. Peyser, A.E. Vinson, A.P. Bartko, R.M. Dickson, Photoactivated fluorescence

from individual silver nanoclusters, Science . 291 (2001) 103–106.

[10] Y.-C. Jao, M.-K. Chen, S.-Y. Lin, Enhanced quantum yield of dendrimer-entrapped gold nanodots by a specific ion-pair association and microwave irradiation for bioimaging, Chem. Commun. 46 (2010) 2626–2628.

[11] C.-A.J. Lin, T.-Y. Yang, C.-H. Lee, S.H. Huang, R.A. Sperling, M. Zanella, J.K. Li, J.-L. Shen, H.-H. Wang, H.-I. Yeh, others, Synthesis, characterization, and bioconjugation of fluorescent gold nanoclusters toward biological labeling applications, ACS Nano. 3 (2009) 395–401.

[12] T. Huang, R.W. Murray, Visible luminescence of water-soluble monolayer-protected gold clusters, J. Phys. Chem. B. 105 (2001) 12498–12502.

[13] J. Zheng, R.M. Dickson, Individual water-soluble dendrimer-encapsulated silver nanodot fluorescence, J. Am. Chem. Soc. 124 (2002) 13982–13983.

[14] W. Guo, J. Yuan, E. Wang, Oligonucleotide-stabilized Ag nanoclusters as novel fluorescence probes for the highly selective and sensitive detection of the Hg2+ ion, Chem. Commun. (2009) 3395–3397.

[15] W. Chen, X. Tu, X. Guo, Fluorescent gold nanoparticles-based fluorescence sensor for Cu2+ ions, Chem. Commun. (2009) 1736–1738.

[16] J. Xie, Y. Zheng, J.Y. Ying, Highly selective and ultrasensitive detection of Hg^{2+} based on fluorescence quenching of Au nanoclusters by Hg^{2+}--Au^{+} interactions, Chem. Commun. 46 (2010) 961–963.

[17] R. Tominaga, M. Sivakumar, M. Tanaka, T. Kinoshita, Visible detection of biotin by thin-film interference: thickness control through exchange reaction of biotin/dethiobiotin-avidin bonding, J. Mater. Chem. 18 (2008) 976–980.

[18] Y.-C. Shiang, C.-C. Huang, H.-T. Chang, Gold nanodot-based luminescent sensor for the detection of hydrogen peroxide and glucose, Chem. Commun. (2009) 3437–3439.

[19] M.A. Li-Na, L.I.U. Dian-Jun, W. Zhen-Xin, Synthesis and applications of gold nanoparticle probes, Chinese J. Anal. Chem. 38 (2010) 1–7.

[20] J. Berg, J. Tymoczko, L. Stryer, Lipids and Cell Membranes, Biochemistry,5 th edition

New York: W H Freeman (2002) 319–344.

[21] E.M. Marti, C. Methivier, P. Dubot, C.M. Pradier, Adsorption of (S)-histidine on Cu (110) and oxygen-covered Cu (110), a combined Fourier transform reflection absorption infrared spectroscopy and force field calculation study, J. Phys. Chem. B. 107 (2003) 10785–10792.

[22] B. Ünal, Z. Durmus, A. Baykal, H. Sözeri, M.S. Toprak, L. Alpsoy, L-Histidine coated iron oxide nanoparticles: synthesis, structural and conductivity characterization, J. Alloys Compd. 505 (2010) 172–178.

[23] M.K. Saha, U. Mukhopadhyay, I. Bernal, Cleavage of the peptide bond of β-alanyl-l-histidine (carnosine) induced by a Co III--amine complexes: reaction, structure and mechanism, Dalt. Trans. (2004) 1466–1473.

[24] R.S. Yadav, P. Mishra, R. Mishra, M. Kumar, A.C. Pandey, Growth mechanism and optical property of CdS nanoparticles synthesized using amino-acid histidine as chelating agent under sonochemical process, Ultrason. Sonochem. 17 (2010) 116–122.

[25] V.G. Sreevalsa, P.P. Jeeju, M.S. Augustine, K.M. Anilkumar, S. Jayalekshmi, L-Histidine-modified biocompatible zinc oxide nanocrystals, J. Exp. Nanosci. 8 (2013) 937–946.

[26] L. Zhou, S. Li, Y. Su, X. Yi, A. Zheng, F. Deng, Interaction between histidine and Zn (II) metal ions over a wide pH as revealed by solid-state NMR spectroscopy and DFT calculations, J. Phys. Chem. B. 117 (2013) 8954–8965.

[27] L.R. Shobin, D. Sastikumar, S. Manivannan, Glycerol mediated synthesis of silver nanowires for room temperature ammonia vapor sensing, Sensors Actuators A Phys. 214 (2014) 74–80.

[28] Y. Ma, H. Niu, Y. Cai, Colorimetric detection of copper ions in tap water during the synthesis of silver/dopamine nanoparticles, Chem. Commun. 47 (2011) 12643–12645.

[29] C. Liao, M. Zhang, L. Niu, Z. Zheng, F. Yan, Organic electrochemical transistors with graphene-modified gate electrodes for highly sensitive and selective dopamine sensors, J. Mater. Chem. B. 2 (2014) 191–200.

[30] Z. Wang, Y. Bai, W. Wei, N. Xia, Y. Du, Magnetic Fe_3O_4-based sandwich-type

biosensor using modified gold nanoparticles as colorimetric probes for the detection of dopamine, Materials. 6 (2013) 5690–5699.

[31] D. Ritheshraj, S. Prasanth, T. V Vineeshkumar, C. Sudarsanakumar, Surface Plasmon Resonance based fiber optic dopamine sensor using green synthesized silver nanoparticles, Sensors Actuators B. Chem. (2015) 224, 600-606.

32] Z. Liu, Y. Zu, Y. Fu, R. Meng, S. Guo, Z. Xing, S. Tan, Hydrothermal synthesis of histidine-functionalized single-crystalline gold nanoparticles and their pH-dependent UV absorption characteristic, Colloids Surfaces B Biointerfaces. 76 (2010) 311–316.

[33] C. Siva, C.N. Iswarya, P. Baraneedharan, M. Sivakumar, L-cysteine assisted formation of mesh like Ag 2 S and Ag 3 AuS 2 nanocrystals through hydrogen bonds, Mater. Lett. 134 (2014) 56–59.

[34] A. Barth, The infrared absorption of amino acid side chains, Prog. Biophys. Mol. Biol. 74 (2000) 141–173.

[35] S.N. Sarangi, A.M.P. Hussain, S.N. Sahu, Strong UV absorption and emission from L-cysteine capped monodispersed gold nanoparticles, Appl. Phys. Lett. 95 (2009) 73109.

[36] J. Xiang, H. Cao, Q. Wu, S. Zhang, X. Zhang, A.A.R. Watt, L-cysteine-assisted synthesis and optical properties of Ag2S nanospheres, J. Phys. Chem. C. 112 (2008) 3580–3584.

[37] Z. Liu, Z. Xing, Y. Zu, S. Tan, L. Zhao, Z. Zhou, T. Sun, Synthesis and characterization of L-histidine capped silver nanoparticles, Mater. Sci. Eng. C. 32 (2012) 811–816.

[38] T.R. Jensen, M.D. Malinsky, C.L. Haynes, R.P. Van Duyne, Nanosphere lithography: tunable localized surface plasmon resonance spectra of silver nanoparticles, J. Phys. Chem. B. 104 (2000) 10549–10556.

List of figures:

Fig 1: UV-Vis absorption spectra recorded at different reaction intervals (A) L-His capped Ag nanoparticles, (B) L-His capped Au nanoparticles, and (C) L-His capped Ag-Au.

Fig 2: (A) FT-IR spectrum of L-His, L-His capped Ag, Au, and Ag-Au nanoparticles. (B) The magnified graph to show symmetric stretching of N-H and COO^{-}.

Fig 3: XRD pattern of L-His capped Ag, Au, and Ag-Au nanoparticles.

Fig 4: AFM 2D and 3D images of L-His capped Ag (A), Au (B) and Ag-Au (C) nanoparticles in the scale of 2 μm.

Fig 5: HR-TEM images of L-His capped Ag nanoparticles (A)&(B), L-His capped Au nanoparticles (D)& (E), L-His capped Ag-Au nanoparticles(G) & (H) respectively in 50 nm and 10 nm scale range. Particle size distribution histogram for L-His capped Ag (C), Au (F) and Ag-Au (I) nanoparticles.

Fig 6: HR-TEM images and SAED pattern for L-His capped Ag (A), Au (B) and Ag-Au (C) nanoparticles.

Fig 7: Formation mechanism of L-His capped Ag nanoparticle.

Fig 8: UV-Vis spectra of DA added at various concentration of (A) L-His capped Ag nanoparticles, (C) L-His capped Au nanoparticles, (E) L-His capped Ag-Au nanoparticles and (B), (D), (F) shows the graph between Logarithmic concentration of DA with wavelength and absorbance intensity of L-His capped Ag, Au, and Ag-Au respectively.

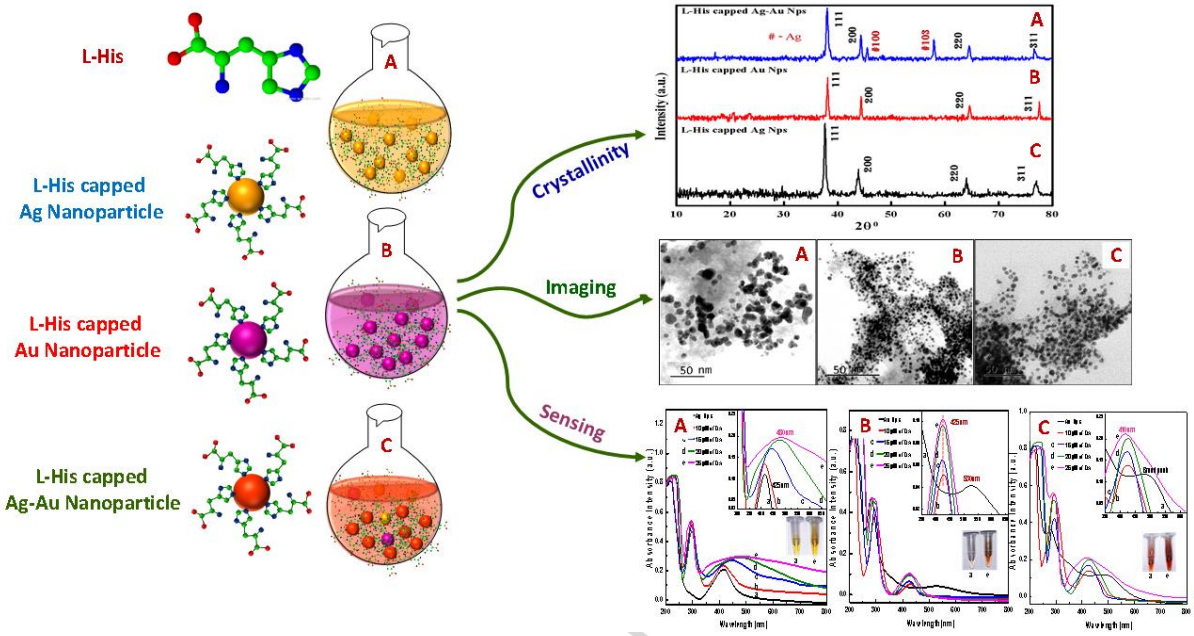

Graphical abstract

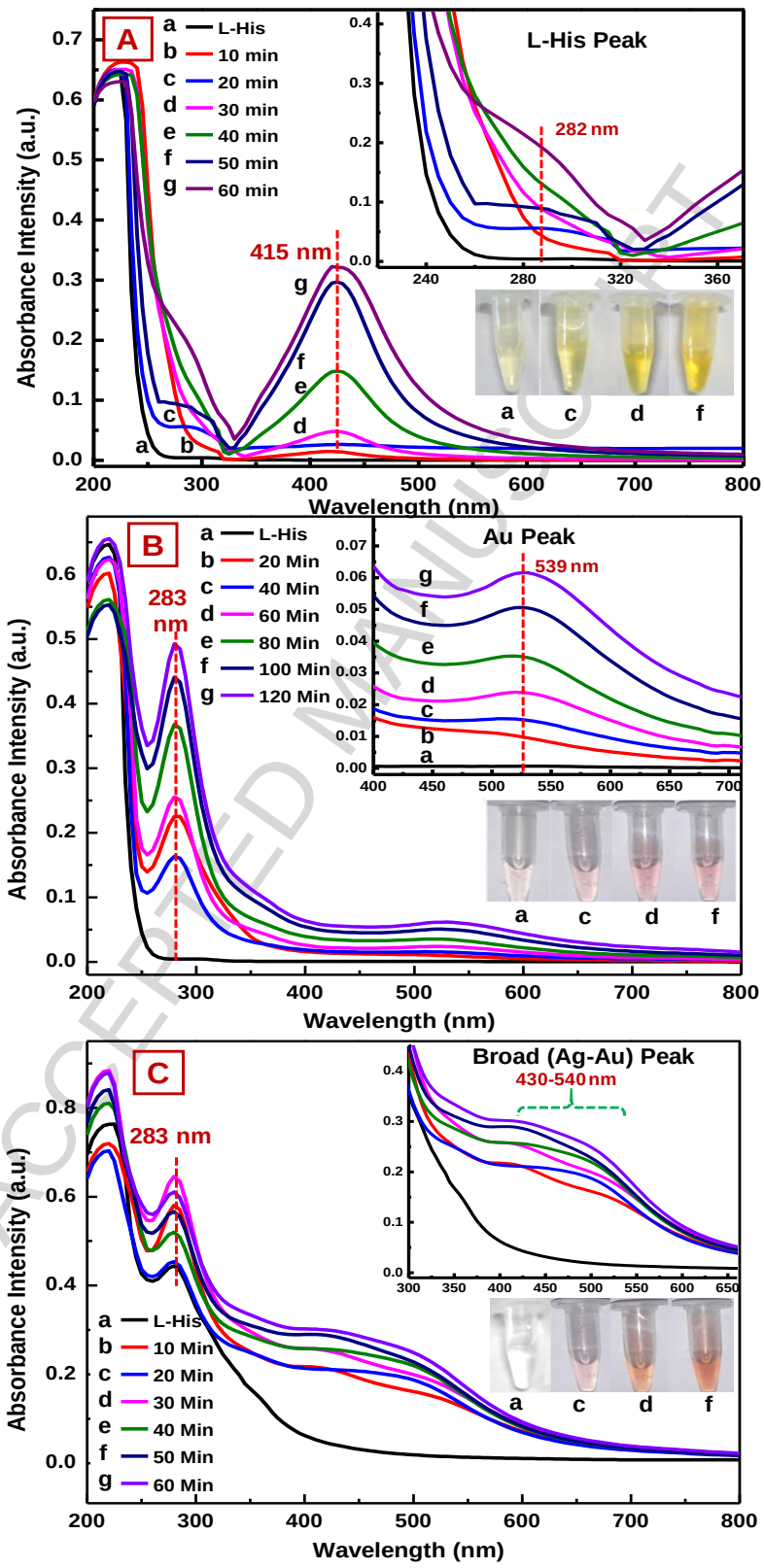

Fig 1: UV-Vis absorption spectra recorded at different reaction intervals (A) L-His capped Ag nanoparticles, (B) L-His capped Au nanoparticles, and (C) L-His capped Ag-Au nanoparticles.

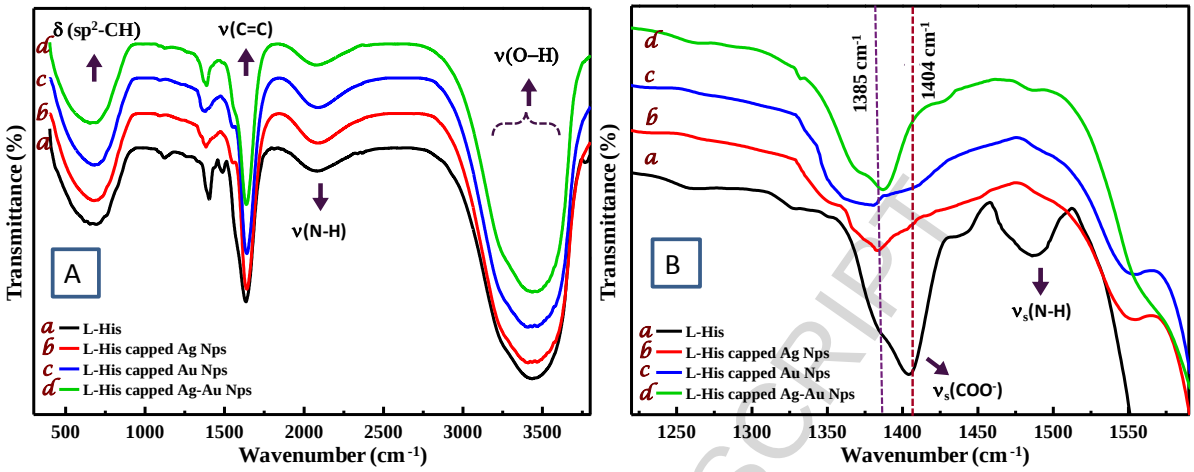

Fig 2: (A) FT-IR spectrum of L-His, L-His capped Ag, Au and Ag-Au nanoparticle. (B) Magnified graph to show symmetric stretching of N-H and COO^{-}

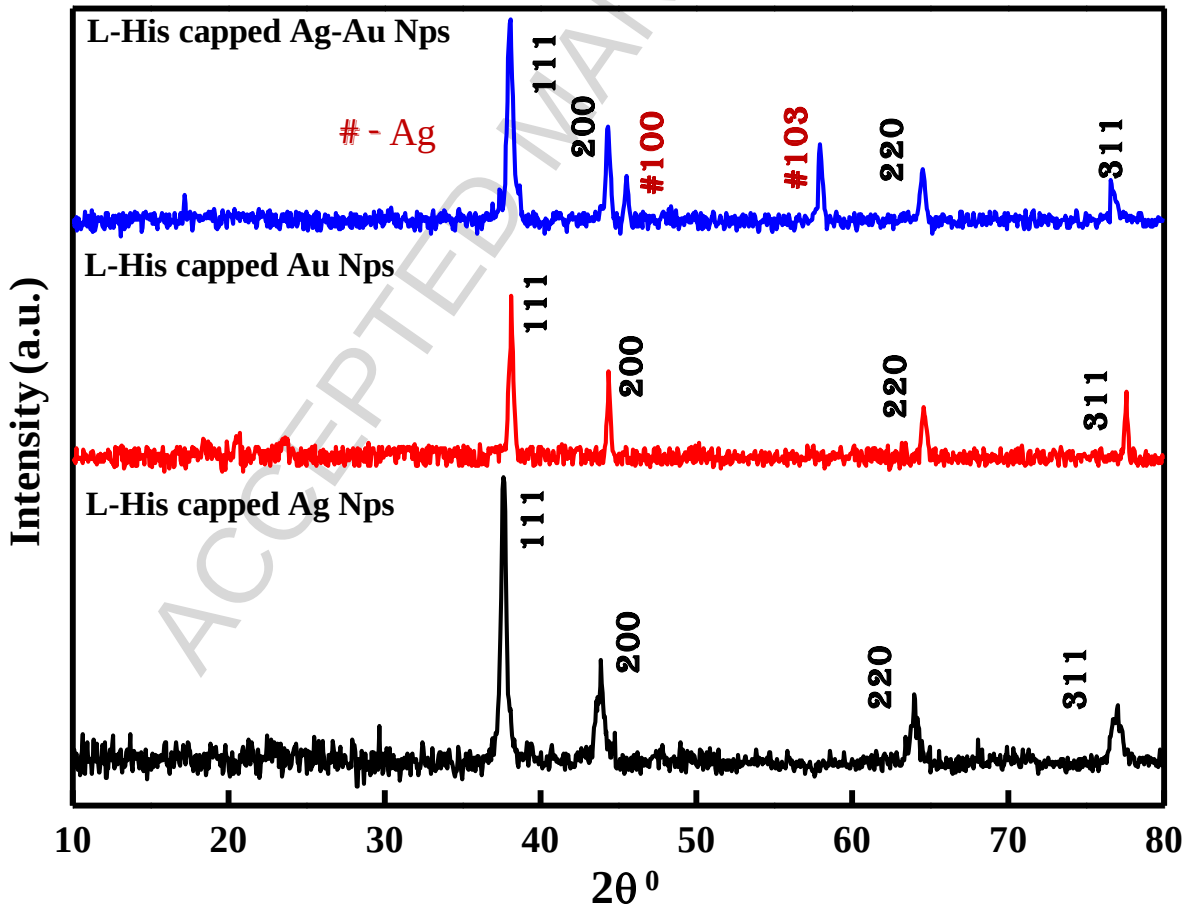

Fig 3: XRD pattern of L-His capped Ag, Au and Ag-Au nanoparticles.

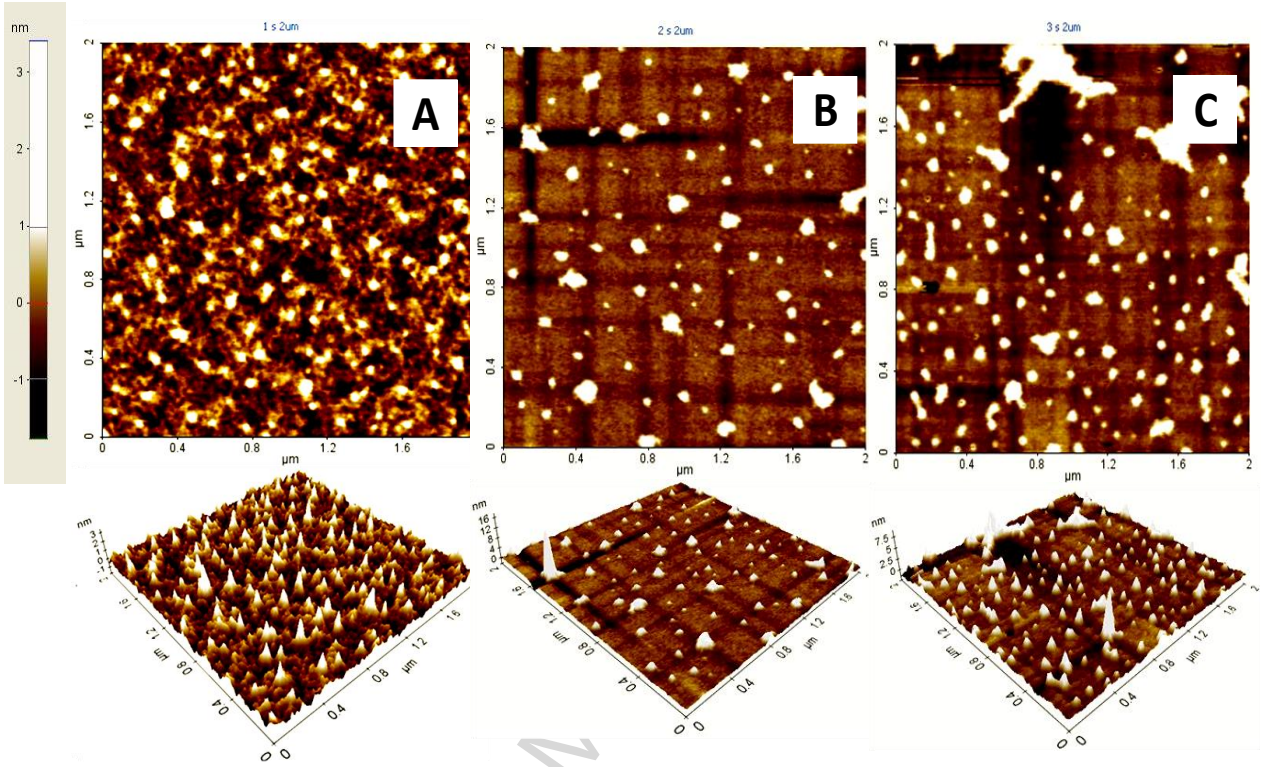

Fig 4: AFM 2D and 3D images of L-His capped Ag (A), Au (B) and Ag-Au (C) nanoparticles in scale of 2 µm.

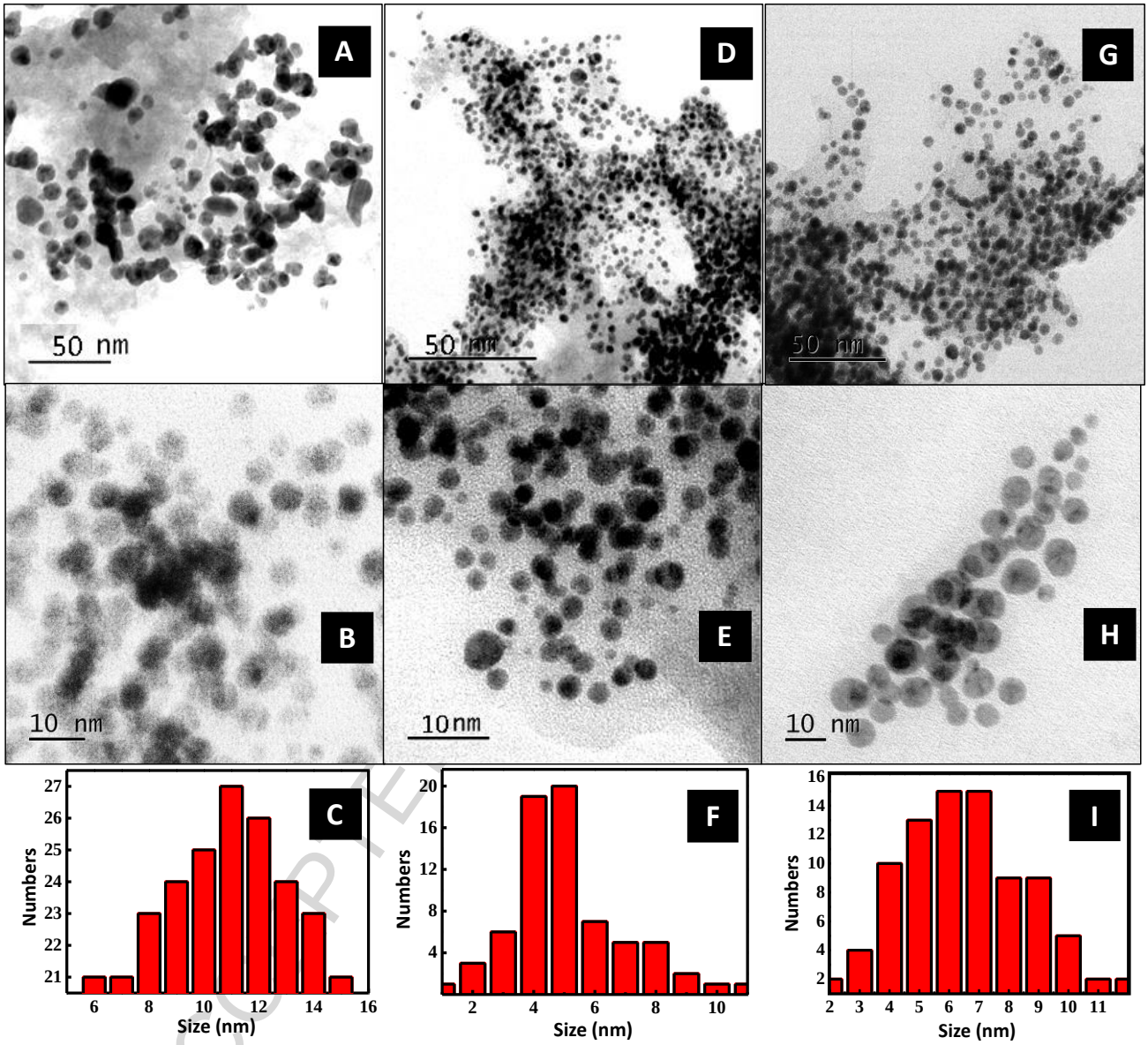

Fig 5: HR-TEM images ofL-His capped Ag nanoparticles (A)&(B), L-His capped Au nanoparticles (D)& (E), L-His capped Ag-Au nanoparticles (G) & (H) respectively in 50 nm and 10 nm scale range. Particle size distribution histogram for L-His capped Ag(C), Au(F) and Ag-Au (I) nanoparticles.

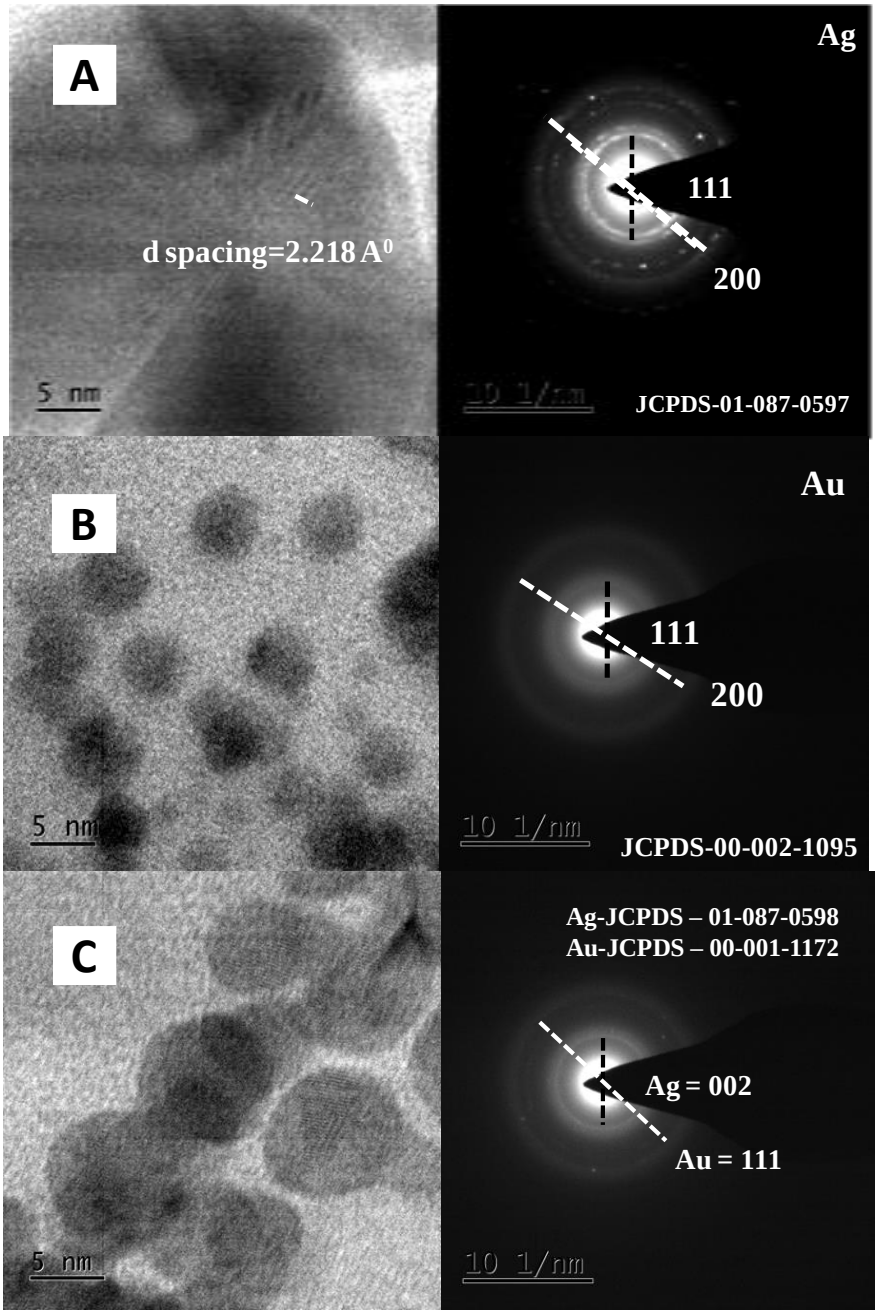

Fig 6: HR-TEM images and SAED pattern for L-His capped Ag (A), Au (B) and Ag-Au (C) nanoparticles.

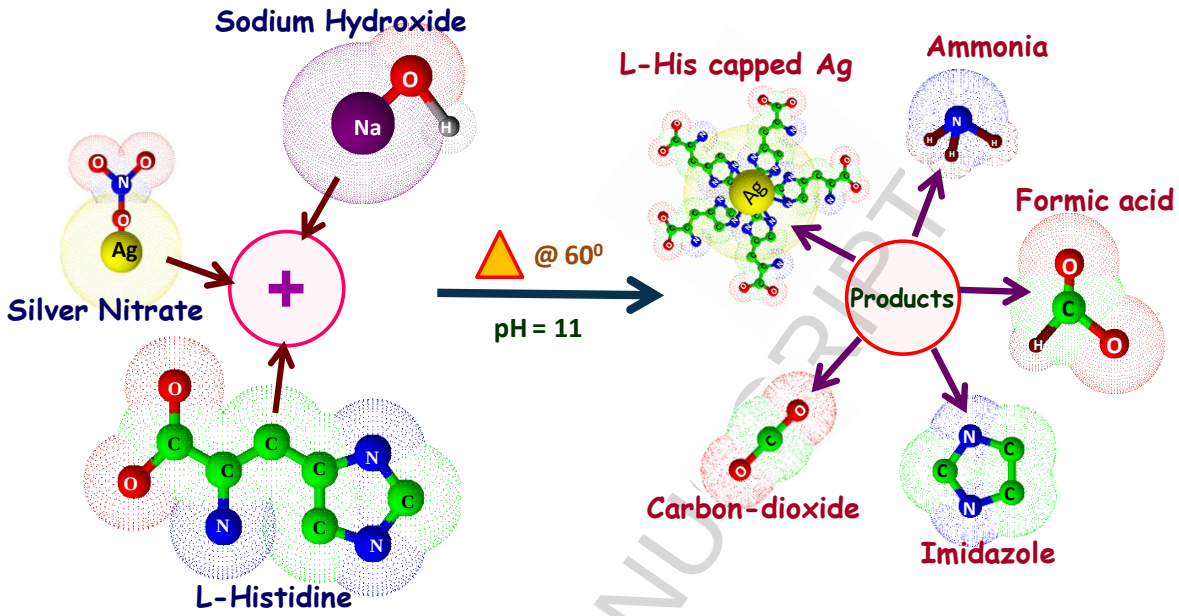

Fig 7: Formation mechanism of L-His capped Ag nanoparticles.

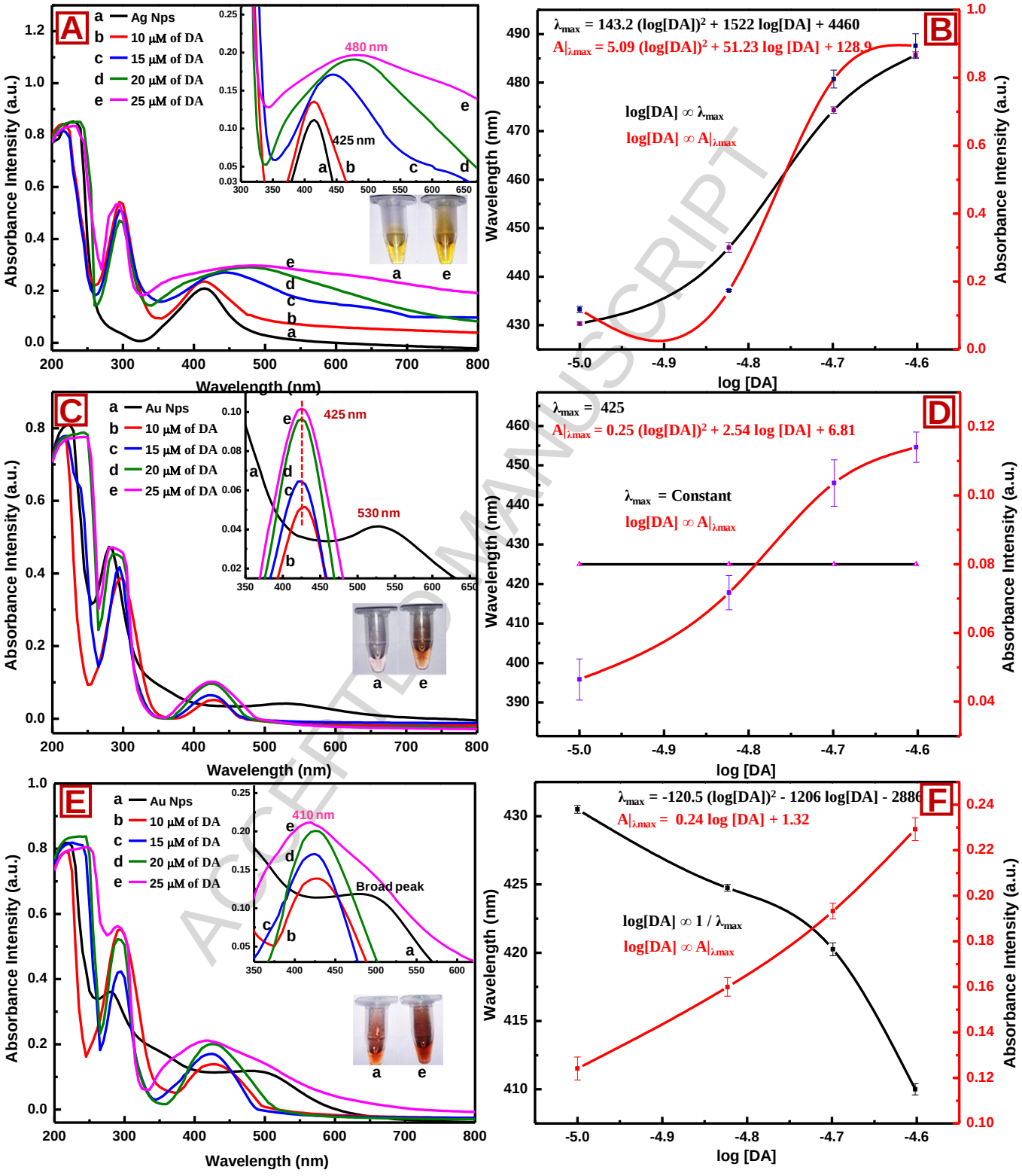

Fig 8: UV-Vis spectra of DA added at various concentration of (A) L-His capped Ag nanoparticles, (C) L-His capped Au nanoparticles, (E) L-His capped Ag-Au nanoparticles and (B), (D), (F) shows the graph between Logarithmic concentration of DA with wavelength and Absorbance intensity of L-His capped Ag, Au and Ag-Au respectively.

HIGHLIGHTS:

1. L-Histidine (L-His) functionalized Ag, Au and bimetallic Ag-Au nanoparticles were prepared by the simple method and its properties were studied
2. L-His based Ag, Au, Ag-Au nanoparticles have characterized by spectroscopy, XRD and microscopic studies.
3. Enhanced optical nature of nanoparticles provides the best platform to develop a colorimetric-based biosensor for dopamine (DA) detection
4. For qualitative determination of dopamine, SPR of metal nanoparticles plays a major role.
5. This basic finding can be utilized for further identification of imbalanced DA concentration in body fluids which cause serious neuro disorder.